Available online at www.sciencedirect.com
SCIENCE DIRECT®
Journal of Chromatography A, 1086 (2005) 141–150
JOURNAL OF CHROMATOGRAPHY A
www.elsevier.com/locate/chroma

Flow regime at ambient outlet pressure and its influence in comprehensive two-dimensional gas chromatography

Jan Beens [a], Hans-Gerd Janssen [b,c], Mohamed Adahchour [a,*], Udo A. Th. Brinkman [a]

[a] *Department of Analytical Chemistry and Applied Spectroscopy, Vrije Universiteit, De Boelelaan 1083, 1081 HV Amsterdam, The Netherlands*
[b] *Advanced Measurement and Imaging, Unilever Research and Development, Olivier van Noortlaan 120, 3133 AT Vlaardingen, The Netherlands*
[c] *Polymer-Analysis Group, Faculty of Science, University of Amsterdam, Nieuwe Achtergracht 166, 1018 WV Amsterdam, The Netherlands*

Available online 11 July 2005

Abstract

With method development in one-dimensional GC already being a tedious task, developing GC × GC methods is even more laborious. The majority of the present GC × GC applications are derived from previously optimised 1D-GC methods, from which especially the carrier gas flow settings are copied. However, in view of the high pressure inside the first-dimension column (high flow resistance of the narrow-bore second-dimension column), diffusion in the first column is much slower than in 1D-GC. Proper optimisation of the column combination and the carrier gas flow can considerably improve separations in GC × GC. To assist in the process of selecting column dimensions and flow rate optimization, we have developed a computer programme, based on Excel®, that enables quick and simple calculation for all types of column combinations. The programme merely needs column dimensions and carrier gas type as input parameters and calculates all resolution and velocity parameters of the GC × GC separation by using flow rate and plate height equations. From the calculations a number of interesting conclusions can be drawn. As an example, the calculations clearly show that the majority of column combinations reported up till now have been operated at a far from optimal flow – and, consequently, a far from optimal resolution. Probably even more important is the conclusion that the majority of column combinations used so far, i.e. those with 100 μm I.D. second-dimension columns, are not necessarily the best choice for GC × GC.
© 2005 Elsevier B.V. All rights reserved.

Keywords: GC × GC; Optimum flow; Column dimensions; Resolution; Modulation criterion; Sample capacity

1. Introduction

Comprehensive two-dimensional gas chromatography (GC × GC) now exists for over a decade. It has been demonstrated that the technique provides highly structured separations with a high degree of resolution produced by an unprecedented peak capacity. Over a hundred interesting GC × GC separations of complex samples from different areas of application have been reported so far [1]. GC × GC is, obviously, on the brink of a widespread acceptance as a separation technique for real samples.

From all papers published so far covering GC × GC, only a limited number have been dedicated to the development of methods and optimisation based on the thermodynamics determining the separation in a GC × GC system. Beens et al. [2] developed a calculation programme with which the outcome of a GC × GC separation can be predicted, Dallüge et al. [1] published optimization procedures and Ong et al. [3] reported on flow measurements for GC × GC separations. But a comprehensive description of the events taking place inside GC × GC columns has not yet been presented.

Method development and column selection in GC × GC is still largely empirical. With trial-and-error method development already being a tedious task in 'normal' one-dimensional GC (1D-GC), it is evident that method development in two-dimensional techniques will be even more laborious. Analogous to 1D-GC, the dimensions and flow settings of the column combination in GC × GC are of utmost importance. The majority of the present GC × GC applications are, however, derived from previously optimized 1D-GC methods, where especially the carrier gas flow

* Corresponding author. Tel.: +31 20 444 7525; fax: +31 20 444 7543.
E-mail address: adahchou@few.vu.nl (M. Adahchour).

0021-9673/$ – see front matter © 2005 Elsevier B.V. All rights reserved.
doi:10.1016/j.chroma.2005.05.086

settings were copied from these methods. But in view of the high pressure level generally encountered in the first column (as a result of the high flow resistance of the narrow-bore, i.e. 100 μm I.D., second-dimension column), diffusion coefficients in the first column and, consequently, also the optimum velocity are far lower than in 1D-GC. Rohwer et al. [4] already indicated that the diffusion inside the high-pressure first column in GC × GC is rather low and that, as a consequence, adapted flow conditions should be used. Careful selection of the column dimensions and the carrier gas flow rate will considerably improve GC × GC separations.

This paper intends to describe the separation phenomena in GC × GC and how they differ from those in 1D-GC, and to provide a simple means to optimize separations in GC × GC. Guidelines will be presented to select column dimensions and optimum carrier-gas flow settings for the coupled-column system. This means that, next to the separation optima, viz. plate height (H) and separation speed, also the necessary number of modulations and sample capacity will be taken into account. The software programme developed to do so is easy to use and only requires the carrier gas type, some solute properties and the column dimensions as input parameters. For the time being it is only applicable for ambient outlet conditions. A second version in which also vacuum outlet conditions can be used, will follow in due course.

2. Theory

Giddings [5] defined the conditions that a separation system has to fulfil in order to be truly multidimensional: (i) the components of a mixture are subject to two or more separation steps or mechanisms, in which their displacements are dependent on different factors, and (ii) when two or more components are substantially separated in any single step, they will always remain separated until the completion of the total separative operation.

As for (i), if all components of a sample pass through the two independent separation columns in GC × GC, this criterion is met. As for (ii), if from a peak as it elutes from the first dimension, the cuts that are made are equal to about 25% of its peak width (at least four cuts over a peak), one may conclude that any substantial separation that has been achieved in the first column will be preserved during the second-dimension separation [6,7].

The second requirement can, in GC × GC, be expressed as follows: if we assume that we have four second-dimension cuts over the width of a first-dimension peak and if we further set the width of a peak at the baseline equal to 6σ, the following equations hold:

$$^2t_r \leq 1.5 \times {}^1\sigma \tag{1}$$

or

$$^2t_0(1 + {}^2k) \leq 1.5{}^1\sigma \tag{2}$$

According to the nomenclature proposed by Schoenmakers et al. [8], $^2t_0$, ^2t_r and ^2k are the dead-time, retention time and retention factor in the second-dimension column, respectively; $^1\sigma$ is the standard deviation of a peak eluting from the first-dimension column. We have used Eq. (1) to define our *modulation criterion*, $^2t_r/{}^1\sigma \leq 1.5$, which has to be fulfilled for a two-dimensional separation.

Below, the procedure to calculate band widths, retention times and plate numbers in coupled-column systems is described. A full mathematical treatment is only possible for isothermal operation. In routine GC × GC, isothermal operation will be applied hardly at all and temperature programming is standard practice. For the latter situation zone broadening can only be estimated. Fortunately, as shown by Schutjes et al. [10], the general conclusions regarding the influence of pressure, column dimensions, flow rates, etc. on band width in programmed operation are identical to those in isothermal operation.

The width of the bands eluting from the first-dimension column, $^1\sigma$, if operated under isothermal conditions, is given by:

$$^1\sigma = \sqrt{\frac{^1H\,{}^1t_r^2}{^1L}} \tag{3}$$

Here ^1H is the plate height and ^1L the length of the first-dimension column; ^1t_r is the retention time in the first column. ^1H can be written as [9]:

$$^1H = \frac{1}{^1\mathrm{CE}}\left(\left(\frac{2\,{}^1D_{\mathrm{m,o}}}{^1u_\mathrm{o}} + \frac{f(^1k)\,{}^1d_\mathrm{c}^2\,{}^1u_0}{^1D_{\mathrm{m,o}}}\right){}^1f_1 + \frac{g(^1k)\,{}^1d_\mathrm{f}^2\,{}^1u_o\,{}^1f_2}{^1D_\mathrm{s}}\right) \tag{4}$$

Here $^1D_{\mathrm{m,o}}$ is the analyte diffusion coefficient in the mobile phase in the first-dimension column under column outlet conditions, i.e. at the modulator. $^1u_\mathrm{o}$ is the outlet linear velocity of the first column, i.e. the velocity at the modulator pressure, $^1d_\mathrm{c}$ is the diameter of the first column, $^1d_\mathrm{f}$ the stationary phase film thickness of the first-dimension column and $^1D_\mathrm{s}$ the analyte diffusion coefficient in the stationary phase in the first column. ^{1}CE is the coating efficiency of the first column, and $f(^1k)$ and $g(^1k)$ are functions of the retention factor:

$$f(^1k) = \frac{(1 + 6\,{}^1k + 11\,{}^1k^2)}{96(1 + {}^1k)^2} \tag{5}$$

and

$$g(^1k) = \frac{2\,{}^1k}{3(1 + {}^1k)^2} \tag{6}$$

$^1f_1$ and $^1f_2$ are pressure correction factors [11]:

$$^1f_1 = \frac{9(^1p_\mathrm{o}^4 - 1)(^1p_\mathrm{o}^2 - 1)}{8(^1p_\mathrm{o}^3 - 1)^2} \tag{7}$$

and

$$ {}^1f_2 = \frac{3({}^1p_o^2 - 1)}{2({}^1p_o^3 - 1)} \quad (8) $$

where:

$$ {}^1p_o = \frac{{}^1p_{in}}{{}^1p_{out}} \quad (9) $$

Here ${}^1p_{in}$ and ${}^1p_{out}$ are the inlet and outlet pressures of the first-dimension column, respectively. For the second-dimension column the equations describing band width and plate height are analogous.

All parameters in Eqs. (1)–(9) are relatively easy to obtain, with the exception of ${}^1p_{out}$ (which is identical to ${}^2p_{in}$). ${}^1p_{out}$ or ${}^2p_{in}$ is the midpoint pressure, i.e. the pressure in the modulator of the coupled-column set. Knowledge of this pressure is crucial to describe the flows in both columns. Because it cannot be measured nor calculated directly, a detailed insight in the gas flows in GC × GC columns was never available. To provide it, we have to consider that this pressure can be calculated indirectly from the inlet and outlet pressure of the column combination using the Poiseuille equation and the fact that the mass flow through both columns is the same (columns are coupled in series). According to the Poiseuille equation, the volumetric flow rate through the first-dimension column is equal to:

$$ {}^1F = \left(\frac{\pi {}^1d_c^4}{256\eta {}^1L}\right)\left(\frac{{}^1P_{in}^2 - {}^1p_{out}^2}{{}^1p_{out}}\right)\left(\frac{T_{mod}}{{}^1T}\right) \quad (10) $$

Here ${}^1F$ is the volumetric flow through the first-dimension column under modulator conditions, η is the dynamic viscosity of the carrier gas and T_{mod} and ${}^1T$ are the temperatures in the modulator and first-dimension column, respectively.

For the second-dimension column the equation is slightly different:

$$ {}^2F = \left(\frac{\pi {}^2d_c^4}{256\eta^2 L}\right)\left(\frac{{}^2p_{in}^2 - {}^2p_{out}^2}{{}^2p_{out}^2}\right)\left(\frac{T_{mod}}{{}^2T}\right)\left(\frac{{}^2p_{out}}{{}^1p_{out}}\right) \quad (11) $$

Here the additional term $({}^2p_{out}/{}^1p_{out})$ is needed to convert the velocity in the second-dimension column to modulator conditions. Under steady-state conditions ${}^1F$ is equal to ${}^2F$. If we further assume that the temperature in the two columns and the modulator is the same, Eqs. (10) and (11) can be combined to give:

$$ \left(\frac{{}^1d_c^4}{{}^1L}\right)\left(\frac{{}^1p_{in}^2 - {}^1p_{out}^2}{{}^1p_{out}}\right) = \left(\frac{{}^2d_c^4}{{}^2L}\right)\left(\frac{{}^2p_{in}^2 - {}^2p_{out}^2}{{}^2p_{out}}\right)\left(\frac{{}^2p_{out}}{{}^1p_{out}}\right) \quad (12) $$

After some rewriting we finally obtain:

$$ {}^1p_{out}^2 = \frac{{}^1d_c^4\,{}^2L\,{}^1p_{in}^2 + {}^2d_c^4\,{}^1L\,{}^2p_{out}^2}{{}^2d_c^4\,{}^1L + {}^1d_c^4\,{}^2L^2} \quad (13) $$

Since we now know the in- and output pressures of both columns, the average linear velocities and the residence times can be calculated from:

$$ {}^1u_o = \frac{{}^1F}{(\pi/4){}^1d_c^2} \quad (14) $$

to be

$$ {}^1\bar{u} = {}^1u_o\,{}^1f_2 \quad (15) $$

and

$$ {}^1t_r = \frac{{}^1L(1 + {}^1k)}{{}^1\bar{u}} \quad (16) $$

where ${}^1\bar{u}$ is the average linear velocity in the first-dimension column. Identical equations hold for the second-dimension column.

From the above equations we can calculate the plate height curves and band widths in GC × GC. To this end a computer programme was written in Microsoft Excel®. The required viscosities were calculated from the equations given by Ettre [12]; stationary-phase diffusion coefficients were calculated from [13]:

$$ D_s = \frac{D_m}{50\,000} \quad (17) $$

${}^1D_{m,o}$ was calculated from:

$$ {}^1D_{m,o} = \frac{{}^2D_{m,o}\,{}^2p_{out}}{{}^1p_{out}} \quad (18) $$

Here ${}^2D_{m,o}$, the analyte diffusion coefficient in the mobile phase at atmospheric outlet pressure, was obtained from the models proposed by Fuller et al. [14].

3. Experimental

3.1. Chemicals and samples

Solutions of dodecane and benzothiophene were made in freshly distilled hexane (J.T. Baker, Deventer, the Netherlands) at a concentration of 10 μg/mL.

Olive oil extracts in diethyl ether or in pentane were obtained from Unilever Research and Development (Vlaardingen, the Netherlands). High-vacuum degassing (HVD), which is a suitable technique to isolate flavour compounds from fat or oily matrices under mild conditions, was used to isolate the volatile flavours from the extract [15]. The olive oil samples were subjected to HVD at room temperature and under high vacuum (1.6×10^{-6} mbar). After 5 h of extraction, the solid material trapped by means of liquid nitrogen (−185 °C) was dissolved in 2 mL of diethyl ether or

pentane. In order to avoid losses of volatiles, 1 μL of each final extract was injected in the GC system without any pre-concentration.

3.2. GC × GC conditions

The gas chromatograph used was a Hewlett-Packard HP6890 (Agilent, Palo Alto, CA, USA) instrument with a split/splitless injector and a flame ionisation detection system (FID) capable of producing a digital signal at a rate of 200 Hz. The 15.5 m × 0.25 mm I.D. first-dimension column was coated with a 0.25-μm film of BPX-5 (SGE Europe, Milton Keynes, UK). Through a press-fit connector it was coupled to the 1 m × 0.1 mm I.D. second-dimension column, which was coated with 0.1 μm of BPX50 (SGE Europe).

The carrier gas was helium (99.999% purity; Hoekloos, Schiedam, the Netherlands). For the determination of $H/\bar{u}$ curves, isothermal runs (100 °C) were performed by injecting 1 μL of the standard solution and varying the head pressure of the first column between 50 and 690 kPa, which is the maximum pressure that could be applied. The olive oil extract was analysed by applying three selected head pressures, viz. 100, 200 and 300 kPa (see below). The temperature of the two GC columns, which were housed in the same oven, was programmed from 40 °C (2 min hold) to 180 °C (0.33 min hold) at 3 °C/min and, next, to 280 °C at 20 °C/min.

A dual-stage cryogenic jet modulator [16] was used at a modulation time of 4 s.

A Hewlett-Packard Chemstation was applied for data acquisition. For data transformation and visualization two additional programmes were used, a programme to convert the raw data into a two-dimensional array (Ph. J. Marriott, Melbourne, Australia) and a programme to generate contour plots from this array ("Transform", part of Noesys software package; Research Systems International, Crowthorne, UK).

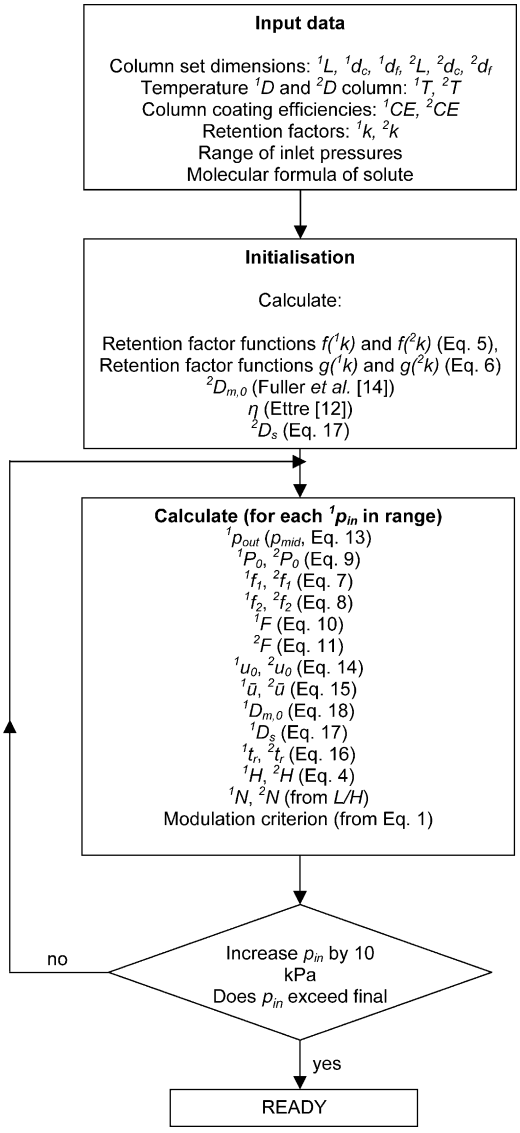

Fig. 1. Algorithm for the calculation of $H/\bar{u}$ curves and related parameters for GC × GC column sets for a range of inlet pressures.

4. Results and discussion

4.1. The computer model

The computer programme calculates the plate height at a specific inlet pressure, $^1p_{in}$, and a constant ensemble outlet pressure, $^2p_{out}$, of 1 bar (flame ionisation detection). First, the programme calculates $^1p_{out}$ using Eq. (13). Next, Eqs. (7)–(9) provide the pressure correction factors. The volumetric flow rates are calculated from Eqs. (10) or (11). The corresponding average linear velocities are calculated through Eqs. (14) and (15). Eq. (18) finally gives the analyte diffusion coefficient for the first column under column-outlet conditions. All these values can now be substituted into Eq. (4) to give the plate height for the first-dimension column (once ^1k and ^{1}CE have been set). By using the corresponding equations and values for the second-dimension column, the second-dimension velocity and plate height are obtained simultaneously. This series of calculations yields one point of the respective $H/\bar{u}$ curves. The programme can automatically calculate a series of these points within a given minimum-to-maximum input pressure range. The plate heights, ^1H and ^2H, will then be plotted versus the average linear velocities. As will be demonstrated below, it is more practical to plot the plate heights versus the inlet pressures (of the column combination) than against the individual velocities, because the velocities in the two columns generally are rather different. Residence times in the two columns are obtained from Eq. (16). Substitution of the values for H, L and t_r in Eq. (3) allows calculation of the band width of the peaks eluting from the first- and second-dimension columns. With these, the modulation criterion can be calculated. Fig. 1 depicts the flow scheme of the software programme. The software provides all such calculations and plots in a very short period of time, typically on the order of few seconds for the calculations reported in Tables 1 and 2.

Table 1
Comparison of performance parameters of six GC × GC column-dimension combinations operated at the optimum flow settings of the first-dimension column

Dimensions of second-dimension column[a] (m × mm I.D., μm d_f)	p_{in} (kPa)	p_{mid} (kPa)	$^1\bar{u}$ (cm s^{-1})	$^2\bar{u}$ (cm s^{-1})	^1N	^2N	$^1N/s$ (s^{-1})	$^2N/s$ (s^{-1})	$^2t_R/^1\sigma$
0.5 × 0.05, 0.05	655	625	8	310	131 000	3800	360	23 300	0.2
1.0 × 0.10, 0.10	305	240	19	180	130 000	7100	820	12 900	1.3
	210[b]	*170*[b]	*11*[b]	*95*[b]	*91 500*[b]	*10 500*[b]	340[b]	*10 150*[b]	*1.2*[b]
1.8 × 0.18, 0.18	235	135	28	85	127 000	10 000	1190	4800	7.0
	210[b]	*130*[b]	*23*[b]	*70*[b]	*123 400*[b]	*10 600*[b]	930[b]	*3800*[b]	*7.3*[b]
2.5 × 0.25, 0.25	225	115	31	50	126 000	10 700	1280	2120	18
	280[c]	*120*[c]	*39*[c]	*75*[c]	*126 000*[c]	*9600*[c]	*1460*[c]	*2830*[c]	*14*[c]
	320[c]	*125*[c]	*42*[c]	90[c]	*126 000*[c]	*8600*[c]	*1420*[c]	*3050*[c]	*11*[c]
3.2 × 0.32, 0.32	215	110	31	30	125 000	10 300	1240	930	38
5.3 × 0.53, 0.53	215	100	31	10	125 000	8200	1290	175	175

[a] First-dimension column, 30 m × 0.25 mm I.D. × 0.25 μm d_f. For abbreviations and symbols, see Fig. 1 and Section 2.
[b] Performance parameters of the column set operated at the optimum flow settings of the second-dimension column.
[c] 33.6 and 37.3 m First-dimension columns operated slightly above their optima to keep ^1N constant at 126 000. For details, see text.

4.2. Validation of the computer model against experimental data

The software programme discussed above has three versions, viz. for hydrogen, helium and nitrogen as the carrier gas. It only requires the column dimensions with its respective coating efficiencies, the molecular structure of the analyte and its retention factors on both columns as the input parameters. As discussed above, from these input values it rapidly calculates the output parameters with which the performance of any column combination can be described.

In order to check whether our programme predicts correct results, we compared for one carrier gas, helium, the experimental $H/\bar{u}$ curves obtained using the benzothiophene peaks recorded for the GC × GC column set with the values acquired from the programme. The details of the column set are given in Experimental. The peak widths of benzothiophene on the first column were determined with the same column set, but now without using the modulator. The influence of the very fast second-dimension column on the final peak shape is negligible. The results of Fig. 2 show that the calculated and experimental $H/\bar{u}$ curves closely agree for both the first- and the second-dimension column. For the column set chosen (15 m × 0.25 mm I.D., 0.25 μm d_f) × (1 m × 0.1 mm I.D., 0.1 μm d_f), the optimum first-dimension average velocity was 20.5 cm s^{-1} (N = 65 000). It should be noted that a range of 17–24 cm s^{-1} can be selected without too much loss of separation power, since at least 96% of the available plates are then generated. It is, however, advisable to select a low velocity, e.g. 18–19 cm s^{-1}, because that is favourable for the second-dimension separation: the second-dimension column is then operated nearer to its optimum.

4.3. Column optimization

When optimizing a GC × GC column set, the separations in the first and second-dimension column should, if possible, both be optimized. In addition, the modulation criterion should be fulfilled in order to preserve the separation of the first column in the second-dimension separation (c.f. Section 2).

The computer programme provides a complete picture of the behaviour of a GC × GC column set as a result of the flow regime and indicates the optima. We therefore, subjected a very popular GC × GC set of column dimensions – (15 m × 0.25 mm I.D., 0.25 μm d_f) × (1.5 m × 0.1 mm I.D.,

Table 2
Comparison of performance parameters of twelve GC × GC column-dimension combinations operated at optimum flow settings of the first-dimension column[a]

Dimensions of column combination (m × mm I.D., μm d_f)	p_{in} (kPa)	p_{mid} (kPa)	$^1\bar{u}$ (cm s^{-1})	$^2\bar{u}$ (cm s^{-1})	^1N	^2N	$^1N/s$ (s^{-1})	$^2N/s$ (s^{-1})	$^2t_R/^1\sigma$
15 × 0.25 × 0.25 + 1.5 × 0.15, 0.15 + 1.8 × 0.18, 0.18	200	150	28	108	64 400	9500	1200	6800	6.5
	190	135	32	86	64 000	10 000	1370	4800	11.3
25 × 0.25 × 0.25 + 1.5 × 0.15, 0.15 + 1.8 × 0.18, 0.18	230	153	26	109	106 800	9500	1100	6850	4.7
	220	135	29	85	106 100	10 000	1230	4750	8.0
20 × 0.32 × 0.32 + 1.5 × 0.15, 0.15 + 1.8 × 0.18, 0.18	200	170	22	140	67 400	7900	760	7300	3.2
	170	140	23	94	66 800	9500	790	5050	5.7
30 × 0.32 × 0.32 + 1.5 × 0.15, 0.15 + 1.8 × 0.18, 0.18	210	165	21	133	100 900	8200	700	7250	2.5
	190	140	23	102	100 400	9200	790	5200	4.4
30 × 0.53 × 0.53 + 1.5 × 0.15, 0.15 + 1.8 × 0.18, 0.18	210	200	12	200	61 250	5300	250	7200	0.7
	170	160	14	150	61 000	6700	280	5600	1.4
50 × 0.53 × 0.53 + 1.5 × 0.15, 0.15 + 1.8 × 0.18, 0.18	210	195	11	190	102 000	5700	240	7200	0.6
	180	164	14	156	101 800	6500	280	5600	1.0

[a] For an explanation of the abbreviations and symbols, see Table 1.

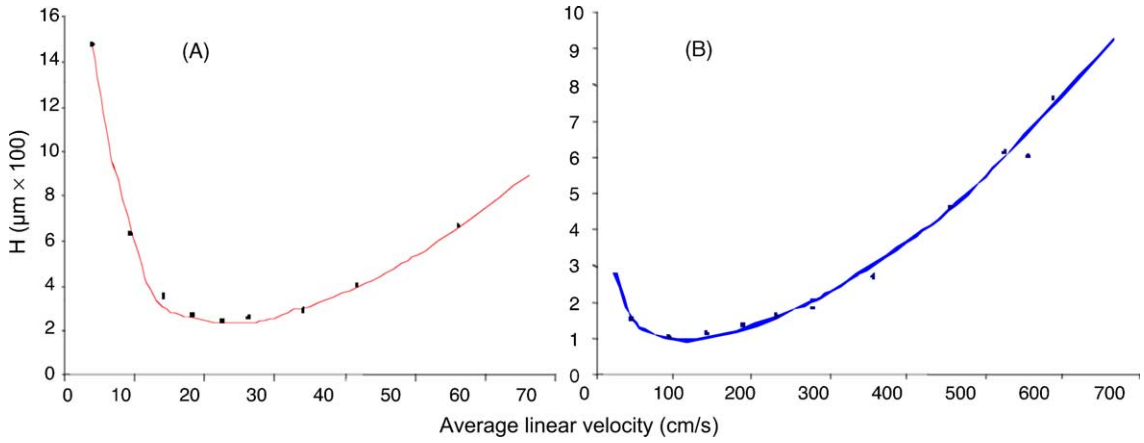

Fig. 2. Comparison of experimental and calculated data for $H/\bar{u}$ curves on the GC × GC column set specified in Experimental, with benzothiophene as analyte and helium as carrier gas. ^{1}CE and ^{2}CE are 90%. (A) first column; (B) second-dimension column. The drawn coloured lines depict the calculated, and the black dots the experimental values.

0.1 μm d_f), used in over 80% of all published separations - to the programme in order to understand its performance. In order to be able to incorporate the curves of both columns in one figure, and to simplify the presentation, the curves are presented as N versus p_{in} curves. From the results depicted in Fig. 3 two important conclusions can be drawn: (i) the optima of both columns are at widely different input pressures and (ii) the optimum of the first column is at a relatively low linear velocity.

The lower optimal linear velocity of the first column in Fig. 3 (compared to Fig. 2) is the result of using a longer second-dimension column, and, therefore, the rather high

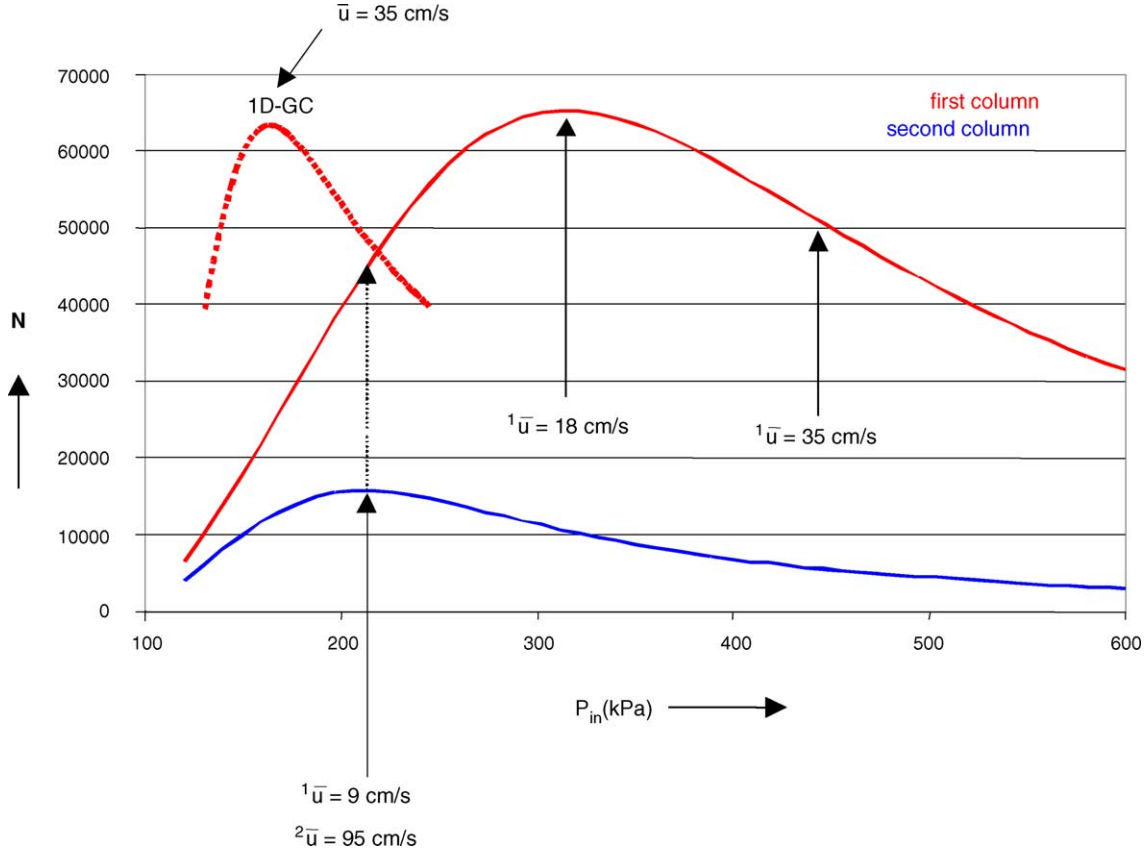

Fig. 3. N vs. p_{in} curves for (15 m × 0.25 mm I.D., 0.25 μm d_f) × (1.5 m × 0.1 mm I.D., 0.1 μm d_f) column combination. Carrier gas, helium. The red line is the curve for the first, and the blue line that for the second-dimension column. The dotted red line is the curve for the first column when used as a 1D-GC column. The arrows depict the points where the average linear velocities in the first column were calculated as indicated.

midpoint pressure. This means that the total pressure in the first column is far higher than when it is used for 1D-GC. Consequently, since analyte diffusion is inversely proportional to pressure, the separation process in the first column is rather slow. This is evident from the calculated values of the average linear velocity in the optima of the curves. The average linear velocity at the optimum of the first-dimension column is 18 cm s^{-1} instead of the normal optimum velocity of 35 cm s^{-1} if the same column is used as a single column in 1D-GC.

Calculations made by using our software programme showed that the modulation criterion of Eq. (1) is met only in a very narrow region, viz. where $p_{in} < 135$ kPa. This corresponds to an unacceptably low average linear velocity, i.e. 3.5 cm s^{-1}. This is highly disadvantageous since it causes, next to an excessively long analysis time, (very) inefficient separations in both dimensions, as is evident from Fig. 3.

In order not to make the first-dimension run too long, most published papers use higher velocities by applying higher input pressures to create, if possible, the necessary peak broadening and, thus, to meet the modulation criterion-demand. However, experience shows that such broadening – generated when the normal optimum velocity of 35 cm s^{-1} as in 1D-GC, is used – does not suffice to reach the goal, certainly not when an optimized temperature-programming rate of 10 °C/void time is used. In other words, it is necessary to further broaden the first-dimension peaks, which can be achieved by decreasing the temperature-programming rate to 2–3 °C/min, a range often used in GC × GC practice. When assuming the optimum programming rate to be 10 °C/void time, the optimum rate can be calculated to be approx. 7 °C/min. Generally speaking, and certainly also for situations such as described in Fig. 3, such a reduced programming rate will have the beneficial effect of creating peaks widths for which the modulation criterion will be met. However, by doing so the first-dimension separation is far below its optimum. As a consequence, in many publications in which column combinations with dimensions similar to the above have been used, next to a not optimal temperature-programming rate, also linear velocities were applied far above the optima calculated by our programme.

For an optimum use of the separation power of the GC × GC column set, one will have to find a compromise. One approach is to operate the first column in its optimum; the plate number of the second-dimension column will then be far below its maximum, albeit that the second-dimension column will have the necessary speed. If, on the other hand, one prefers to operate the second-dimension column in its optimum, the price to pay is not only a low plate number in the first dimension, but also a long analysis time. In order to demonstrate the consequences of different velocities, we compared the chromatograms of an olive oil extract obtained at the three velocities of interest, viz. 9 cm s^{-1} (optimum velocity in second-dimension column), 18 cm s^{-1} (optimum velocity in first-dimension column) and 35 cm s^{-1} (optimum as derived from 1D-GC). The results are depicted in Fig. 4.

The three chromatograms in the top row show the overall separation, while the chromatograms in the centre and bottom rows illustrate details of the first- and second-dimension separations, respectively. It should be emphasized that the chromatograms in the centre row are 1D-GC results using the column set, but without modulation - the modulator is off. Under these conditions (c.f. above), the optimum average linear velocity of the first column is 18 cm s^{-1} (approx. 300 kPa input pressure). The beneficial effect is nicely demonstrated in the central-row chromatogram of Fig. 4b. Separation, especially in the early and final parts (circled regions) of the chromatogram is (much) better than in the other flow situations (Figs. 4a and c). On the other hand, according to Fig. 3 the second-dimension column separation is best at the lowest inlet pressure (200 kPa), as the contour plot (top row) of Fig. 4a convincingly demonstrates. In order to further illustrate this, second-dimension chromatograms across the dashed lines in the contour plots are presented in the bottom row of Fig. 4 and the separation of two co-eluting pairs – marked 1 and 2 – is compared. As expected, their separation in Fig. 4a is much better than in Figs. 4b and c. Finally, the separation on both columns is far from its optimum when the first-dimension velocity of 35 cm s^{-1} (450 kPa input pressure) is applied (Fig. 4c). Both columns are now operated far above their respective optimum velocities and there is a distinct loss of resolution.

The above discussion focuses only on separation quality and does not consider the analysis time, which in a GC × GC separation equals the time of the first-dimension separation. The time ranges indicated on the X-axes of the top row of Fig. 4 ((a) 19–29 min; (b) 14–23 min and (c) 12–20 min) show that the mutual differences are on the order of 5–7 min. That is, they can be considered to be of limited importance when selecting the preferred separation conditions.

4.4. Speed of analysis

In order to illustrate the influence of narrow-bore second-dimension columns on the performance and speed of a GC × GC column set, we calculated the optimum input pressure and resulting separation parameters for a selected set of column combinations. All second-dimension columns were chosen such that they yield about 10 000 theoretical plates when operated under optimum conditions.

The data reported in Table 1 show that, as a result of the high flow resistance of the second-dimension column, the use of 0.05 and 0.10 mm I.D. second-dimension columns results in low optimum linear velocities for the first column, viz. 8 or 19 cm s^{-1}. In other words, the first column now only generates 360 or 820 plates s^{-1}, instead of about 1300 plates s^{-1} as in the other combinations. This will cause a considerable increase of analysis time. Moreover, and possibly more importantly, the linear velocity in the second-dimension column is very high, viz. 180 or even 310 cm s^{-1}. This causes a poor separation performance in the second-dimension

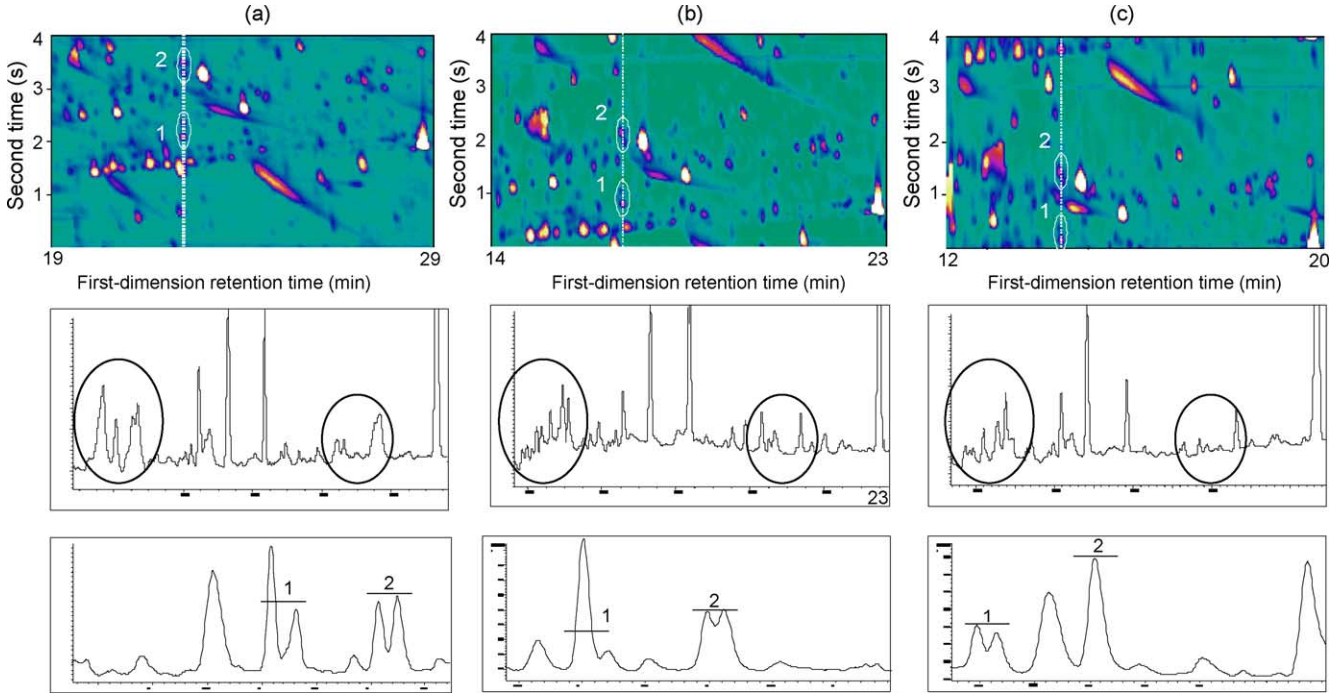

Fig. 4. Details of GC × GC and GC chromatograms of an olive oil extract analysed at an average linear velocity in the first-dimension column of (a) 9 cm s^{-1}, (b) 18 cm s^{-1} and (c) 35 cm s^{-1}. Parts of the contour plots (top), chromatograms depicting the first-dimension separation (centre) and second-dimension chromatograms across the dashed lines in the contour plots (bottom) are shown. The circled areas (centre row) and peak pairs (top and bottom row) are marked to facilitate separation performance in the first dimension and second dimension, respectively. For more details, see text.

column, with 7100 or 3800 instead of the usual 10 000 theoretical plates. From the point of view of analysis time, and also with regard to the quality of the second-dimension separation and sample capacity (see below), the use of 0.05 mm I.D. second-dimension columns should hence be discouraged. For 0.10 mm I.D. second-dimension columns the situation is less extreme but, if a high plate number is needed in the second dimension, the use of a 0.10 mm I.D. column is not the preferred option: the price to pay here is about 3000 theoretical plates in the second-dimension column. If now the second-dimension column is operated at its optimum flow conditions, several consequences have to be considered. As an example, the results for the 0.10 mm I.D. second-dimension column are included in Table 1 (see *a* row). The value of the modulation criterion is seen to improve somewhat, but all other performance parameters are inferior. The average linear velocity in the first-dimension column is now only 11 cm s^{-1}, which is far from its optimum. The reason why no inlet pressure exists where both columns simultaneously yield a close-to-optimum performance is the significant difference in internal diameter of the first- and second-dimension columns. This is demonstrated when a 0.18 instead of a 0.10 mm I.D. second-dimension column is used. As Table 1 indicates, it is better to operate the first- rather than the second-dimension column under optimum flow conditions. In this case, the two columns simultaneously yield close-to-optimum performance. Unfortunately, however, the modulation criterion is still not met at all.

The dilemma one now faces is that, under the present conditions, only the column combinations which use narrow-bore second-dimension columns meet the modulation criterion with values of 1.3–0.2. The three combinations with wider-bore columns, i.e. 0.18, 0.25 and 0.32 mm I.D., only meet the modulation criterion when the peaks eluting from the first column are deliberately broadened, e.g. by applying a very low programming rate. This can be realized more easily for the 0.18 mm I.D. than for the wider columns. However, by doing so, both the first- and second-dimension separations are below their optimum. As for combination with a 0.53 mm I.D. second-dimension column, most probably even the suggested low temperature-programming conditions will fail to bring the very high modulation criterion of 175 down to the required value.

In 1D-GC it sometimes is advantageous to increase the carrier gas flow through the column to a value between the optimum and twice the optimum value. The number of plates generated per unit time is then maximised [18]. In order to evaluate the consequence of working at a slightly above-optimum carrier gas flow in GC × GC, we performed a series of calculations for one of the column sets in Table 1. To compensate for the loss of plates when working at flows above the optimum, the length of the first column was increased to keep the total number of plates constant. Results for the 2.5 m × 0.25 mm × 0.25 μm second-dimension column are included in Table 1 (see *b* row). It is clear that, as in 1D-GC, it is advantageous to work at above-optimum

linear velocities: in both dimensions the number of plates generated per unit time increases. There is a maximum to this increase in speed, as the levelling off of, $^1N/s$ to 1420–1460 s^{-1} for the longer first-dimension columns indicates. As for the second-dimension column, the number of plates generated per time increases while the absolute number of plates decreases. As an example, when the column length is increased from 30 to 37.3 m, $^2N/s$ increases from 2120 to 3050 while ^2N decreases from 10 700 to 8600. The explanation is that the second-dimension separation becomes faster while its efficiency slightly decreases. The absolute plate count, on the other hand, decreases because of the increase of the gas flow above its optimum. For the rest, the modulation criterion is seen to decrease substantially, but the calculated values are still much too high.

4.5. Sample capacity

The sample capacity of a GC × GC system is another aspect of interest. It is well known that narrow-bore columns have a low sample capacity. Ghijsen et al. [17] found that, for columns with equal phase ratios the maximum sample capacity, C_{max}, causing a maximum of 10% peak broadening can be written as:

$$C_{max} \propto \phi d_c^3 \quad (19)$$

where ϕ is a proportionality factor with $0.05 < \phi < 1.8$; $\phi = 1.8$ for solutes and stationary phases with similar chemical functional groups and $\phi = 0.05$ for solutes and stationary phases with very different structures. Sample capacity is thus drastically reduced ($\propto {d_c}^3$) for narrow-bore columns. Moreover, in GC × GC one preferentially selects two columns having widely different separation characteristics, e.g. a polar and a non-polar column. It is therefore expected that ϕ will be unfavourable on one of these columns; obviously this preferably should not be the narrow-bore second-dimension column. One option to increase the sample capacity of the second-dimension column is to use a column with a thicker stationary phase film. However, care should be taken no t to use too thick a film: at phase ratios below approx. 80 the maximum plate number of the columns starts to be affected significantly [19,20]. In this study, only columns with a standard phase ratio of 250 were considered.

From the viewpoint of sample capacity it is clearly advantageous to consider column sets with a relatively wide-I.D. second-dimension column. Moreover, it is obvious that when using 0.25 mm I.D.s in both dimensions, both columns can simultaneously be operated at their optimum velocity. Finally, because the back pressure generated by a not too long second-dimension column of 0.25 mm I.D. is relatively low, the optimal average linear velocity will be close to the optimal velocity of a single 1D-GC column. However, as the pertinent data for a 0.25 mm I.D. column set in Table 1 indicate – although the average linear velocity in the first-dimension column now indeed is as high as 31 cm s^{-1}, the value of the modulation criterion is 18 and, hence, fails by far to meet the specified maximum of 1.5. Scrutiny of the data of Table 1 reveals that accepting a somewhat smaller internal diameter in the second as compared with the first column, i.e. a 0.18 versus 0.25 mm I.D., provides a most acceptable column set. As Table 1 demonstrates, not only can the optima of both columns be reached (nearly) simultaneously (p_{in} optima of 235 and 210 kPa for first- and second-dimension column, respectively), they also exist at relatively high linear velocities, i.e. of 28 and 85 cm s^{-1}, respectively. On the other hand, with a 0.10 mm I.D. column the p_{in} optima are 305 and 210 kPa, respectively. As a consequence, the linear velocity of the first-dimension column is then relatively low, viz. 19 cm s^{-1} and, more importantly, the two columns cannot be simultaneously run at p_{in} values close to their optima. Admittedly, the value of the modulation criterion is distinctly better for the 0.10 mm I.D. as compared with the 0.18 mm I.D. second-dimension column ($^2t_R/^1\sigma$, 1.3 versus 7). However, as mentioned above, operating the system at a low programming rate should suffice to bring the latter value down to ≤1.5: as was also mentioned above, in GC × GC, the programming rate should be, and often is [1], around 3 °C/min, compared to approx. 10 °C/min (column dead time, 1 min) in 1D-GC with a 0.25 mm I.D. column. It is obvious that the sample capacity of the recommended GC × GC column set is substantially higher than that of 'traditional' sets with their 0.10 mm I.D. second-dimension columns.

One might consider to use even wider second-dimension columns than discussed above. This will, however, not bring workable solutions in terms of modulation criterion and separation efficiency. As Table 1 demonstrates, $^2t_R/^1\sigma$ values will be very high, and $^2N/s$, very low. In other words, second-dimension columns should have internal diameters in the 0.10–0.25 mm range. As an illustration, Table 2 presents data calculated for 0.15 and 0.18 mm I.D. second-dimension columns coupled to various first-dimension columns. As for the modulation criterion, its values are seen to be about twice as high for the 0.18 mm I.D. situation, irrespective of the other experimental conditions. Better, i.e. lower, values are found when the internal diameter of the first-dimension column increases. However, this causes the $^1N/s$ values to be very low because of the low linear velocity. In addition, with such column sets the optima of both columns are far from each other and cannot be used simultaneously. Finally, it is interesting to note that with increasing length of the first-dimension column (constant I.D.) not only does ^1N increase as expected, but the value of $^2t_R/^1\sigma$ also distinctly improves.

From the above discussion we may conclude that a good compromise is found when selecting a first-dimension column with a 0.25–0.32 mm I.D., and a second-dimension column with a 0.15–0.18 mm I.D. The length of the first column should be such that enough plates can be generated for the separation at hand (with a relatively long column making it easier to create favourable $^2t_R/^1\sigma$ values). For such sets, the first- and second-dimension columns can be simultaneously run at p_{in} values which are close to the optimum. In addition,

such column sets are fully acceptable regarding the sample capacity issue.

5. Conclusions

A validated computer programme has been developed that allows plate heights and column efficiencies in comprehensive two-dimensional GC to be accurately modelled while using standard plate height and flow equations. The computer programme is available free of charge and will be provided upon request by email. It can conveniently be used to select optimal GC × GC column dimensions and gas flow conditions. Prediction of the various operational parameters and their consequences makes the programme very helpful in method development for GC × GC. On the basis of the calculations in GC × GC at ambient outlet pressure made in the context of the present study, several conclusions can be drawn. These are summarised below.

When optimizing the dimensions of a GC × GC column set, it is advisable to operate both the first- and second-dimension columns close to their optimum gas flows. In principle, this can be achieved by using two columns with the same internal diameter. However, in that case the modulation criterion will be much too high and it will not be easy to bring it down sufficiently, even if the temperature-programming rate is slowed down. Moreover, under these conditions the first- and second-dimension separation efficiency will be sub-optimal.

If two columns with different internal diameters are selected, the various calculations show that one column should be operated close to its optimum flow conditions, and a sub-optimum separation on the other column accepted. The demand made regarding the four modulations across each first-dimension peak, i.e. the modulation criterion, can now be met. Combining a first-dimension column with a 0.25–0.32 mm I.D. with a second one featuring an internal diameter of 0.15–0.18 mm turns out to be a good choice. However, as with the approaches discussed above, some slowing down of the temperature-programming rate is again needed. In other words, the price that has invariably to be paid in GC × GC to arrive at a practicable solution is a time of analysis that is longer than in a comparable 1D-GC analysis. This is mainly the result of slow analyte diffusion in the first column as a result of an increased average column pressure.

Finally, the above recommendations not to use too narrow-I.D. columns in a GC × GC set in either the first or the second dimension, ensure that there will be no undue sample capacity problems.

References

[1] J. Dallüge, R.J.J. Vreuls, J. Beens, U.A.Th. Brinkman, J. Sep. Sci. 25 (2002) 201.
[2] J. Beens, R. Tijssen, J. Blomberg, J. Chromatogr. A 822 (1998) 233.
[3] R. Ong, P. Marriott, P. Morrison, P. Haglund, J. Chromatogr. A 962 (2002) 135.
[4] E.R. Rohwer, W. Welthagen, A. Venter, Presented at the First International Symposium on Comprehensive Multidimensional Gas Chromatography, Volendam, The Netherlands, 2003.
[5] J.C. Giddings, J. High Resolut. Chromatogr. 10 (1987) 319.
[6] R.E. Murphy, M.R. Schure, J.P. Foley, Anal. Chem. 70 (1998) 1585.
[7] J.V. Seeley, J. Chromatogr. A 962 (2002) 21.
[8] P. Schoenmakers, P. Marriott, J. Beens, LC–GC Eur. 16 (2003) 335.
[9] M.J.E. Golay, in: D.H. Desty (Ed.), Gas Chromatography, Butterworths, London, UK, 1958, p. 36.
[10] C.P.M. Schutjes, E.A. Vermeer, J.A. Rijks, C.A. Cramers, J. Chromatogr. 253 (1982) 1.
[11] J.C. Giddings, Dynamics of Chromatography, Part 1, Principles and Theory, Marcel Dekker, New York, 1965.
[12] L.S. Ettre, Chromatographia 18 (1984) 243.
[13] A.E. Scheidegger, The Physics of Flow Through Porous Media, University of Toronto Press, Toronto, 1960.
[14] E.N. Fuller, P.D. Schettler, J.C. Giddings, Ind. Eng. Chem. 58 (1966) 19.
[15] M. Adahchour, L.L.P. van Stee, J. Beens, R.J.J. Vreuls, M.A. Batenburg, U.A.Th. Brinkman, J. Chromatogr. A 1019 (2003) 157.
[16] J. Beens, M. Adahchour, R.J.J. Vreuls, K. van Altena, U.A.Th. Brinkman, J. Chromatogr. A 919 (2001) 127.
[17] R.T. Ghijsen, H. Poppe, J.C. Kraak, P.P.E. Duysters, Chromatographia 27 (1989) 60.
[18] A.J.J. van Es, J.A. Rijks, C.A. Cramers, J. Chromatogr. 477 (1989) 39.
[19] P.A. Leclercq, J. High Resolut. Chromatogr. 15 (1992) 531.
[20] M. van Deursen, H.G. Janssen, J. Beens, P. Lipman, R. Reinierkens, G. Rutten, C. Cramers, J. Microcol. Sep. 12 (2000) 613.